





RESEARCH ARTICLE

The application of unoccupied aerial systems (UAS) for monitoring intertidal oyster density and abundance

Jenny Bueno^{1,2} , Sarah E. Lester^{1,3} , Joshua L. Breithaupt²  & Sandra Brooke² 

¹Department of Geography, Florida State University, Tallahassee, Florida, USA

²Coastal and Marine Laboratory, Florida State University, St. Teresa, Florida, USA

³Department of Biological Science, Florida State University, Tallahassee, Florida, USA

Keywords

Crassostrea virginica, drones, habitat monitoring, high-resolution drone imagery, intertidal oyster reefs, unoccupied aerial systems

Correspondence

Jenny Bueno, Department of Geography, Florida State University, Tallahassee, FL, USA.
E-mail: jbueno@fsu.edu

Funding Information

We gratefully acknowledge the support received from the Triumph Gulf Coast Inc. funding agency through The Apalachicola Bay System Initiative (grant no. 69).

Editor: Dr. Temuulen Sankey
Associate Editor: Dr. Antoine Collin

Received: 12 February 2024; Revised: 14 June 2024; Accepted: 5 July 2024

doi: 10.1002/rse2.417

Abstract

The eastern oyster (*Crassostrea virginica*) is a coastal foundation species currently under threat from anthropogenic activities both globally and in the Apalachicola Bay region of north Florida. Oysters provide numerous ecosystem services, and it is important to establish efficient and reliable methods for their effective monitoring and management. Traditional monitoring techniques, such as quadrat density sampling, can be labor-intensive, destructive of both oysters and reefs, and may be spatially limited. In this study, we demonstrate how unoccupied aerial systems (UAS) can be used to efficiently generate high-resolution geospatial oyster reef condition data over large areas. These data, with appropriate ground truthing and minimal destructive sampling, can be used to effectively monitor the size and abundance of oyster clusters on intertidal reefs. Utilizing structure-from-motion photogrammetry techniques to create three-dimensional topographic models, we reconstructed the distribution, spatial density and size of oyster clusters on intertidal reefs in Apalachicola Bay. Ground truthing revealed 97% accuracy for cluster presence detection by UAS products and we confirmed that live oysters are predominately located within clusters, supporting the use of cluster features to estimate oyster population status. We found a positive significant relationship between cluster size and live oyster counts. These findings allowed us to extract clusters from geospatial products and predict live oyster abundance and spatial density on 138 reefs covering 138 382 m² over two locations. Oyster densities varied between sites, with higher live oyster densities occurring at one site within the Apalachicola Bay bounds, and lower oyster densities in areas adjacent to Apalachicola Bay. Repeated monitoring at one site in 2022 and 2023 revealed a relatively stable oyster density over time. This study demonstrated the successful application of high-resolution drone imagery combined with cluster sampling, providing a repeatable method for mapping and monitoring to inform conservation, restoration and management strategies for intertidal oyster populations.

Introduction

Intertidal oyster habitats are ecologically and economically important in many regions around the world (Beck et al., 2011). Oyster reefs provide several key ecological benefits to estuarine ecosystems. These include providing habitat, food and refuge from desiccation, hypoxia and sedimentation for various species, thereby enhancing

ecosystem biodiversity (Coen et al., 1999; Lenihan & Peterson, 1998; Meyer & Townsend, 2000). Species associated with oyster reefs include economically important transient or resident species of finfish, shrimp and crabs (Coen et al., 1999). Additionally, oyster reefs serve as nurseries for many marine organisms (Coen et al., 1999; Dance et al., 2021). The extensive biogenic structures of reefs can alter water flow and attenuate wave energy,

protecting other habitats, such as salt marshes (Bahr & Lanier, 1981), and human infrastructure from erosion and shoreline retreat (Piazza et al., 2005). Furthermore, oysters can filter large amounts of water, removing particulate matter from the water column and improving water quality for other species, such as seagrasses (zu Ermgassen et al., 2013). Oyster harvesting has also provided food and economic security to coastal communities throughout the world (Beck et al., 2011). Despite these valuable services, an estimated 85% of oyster reefs have been lost globally (Beck et al., 2011), attributed to overharvesting and associated removal of reef structure, coastal development, diseases, changes in freshwater flows and an increase in sediments, nutrients and toxins (Lenihan et al., 1999; Lenihan & Peterson, 1998; MacKenzie et al., 1997).

Given the importance of oyster reefs and their widespread loss and degradation, monitoring programs that assess oyster populations and reef condition are critical for informing management and restoration efforts. Current methods of intertidal oyster reef monitoring include field and aerial imagery surveys. Ground-based surveys can provide estimates of oyster density, sizes and growth (Baggett et al., 2015; Byers et al., 2015; Drexler et al., 2014; Theuerkauf et al., 2017). This involves counting and measuring oysters: juveniles (oysters smaller than 2.5 cm, also referred to as spat), adults (oysters larger than 2.5 cm) and boxes (articulated shell from oysters that have recently died) within a specific quadrat size. However, these surveys can be time-consuming, labor-intensive, destructive and often spatially limited. Alternatively, aerial and satellite imagery can be used for larger scale assessments of reef areal extent and distribution (Benson et al., 2023; Garvis et al., 2015, 2020; Grizzle et al., 2018; Seavey et al., 2011). However, the spatial resolution is often coarse and coordinating image collection with low tides for maximum reef exposure is difficult (Chand & Bollard, 2021; Espriella et al., 2020; Garvis et al., 2020; Gray et al., 2018).

Recent technological advances in unoccupied aerial systems (UAS), also known as drones, complement ground-based surveys, occupied aerial surveys and satellite imagery. These small inexpensive aircraft are increasingly being used for monitoring and ecosystem management (Dronova et al., 2021). For example, UAS can carry small payloads and conduct semi-autonomous or fully autonomous flights, at a much lower cost with greater operational flexibility than occupied systems (Dronova et al., 2021; Klemas, 2015). The images captured from UAS can be used to generate three-dimensional topographic models using structure-from-motion (SfM) photogrammetry techniques (Westoby et al., 2012). SfM requires multiple images that are significantly overlapping to identify and extract features that are matched across

other images. This SfM technique can provide digital elevation models (DEMs), which are digital representations of surfaces containing elevation data. Additionally, SfM can be used to create high-resolution orthomosaics, which are composed of multiple images, free from distortion and referenced to a specified coordinate system. These techniques have been applied to assess topographic variation across marine, estuarine and terrestrial systems (Casella et al., 2017; Joyce et al., 2019; Kalacska et al., 2017; Leon et al., 2015; Ventura et al., 2022). Thus, UAS technology, coupled with SfM techniques, offers a promising tool for oyster reef monitoring by providing high-resolution DEMs and orthomosaics.

The use of UAS has proven effective in mapping and monitoring intertidal wild oyster reefs (Chand & Bollard, 2021; Espriella et al., 2020; Ridge et al., 2020; Windle et al., 2019), and oyster farms (Román et al., 2023). For instance, UAS geospatial products have been combined with automated classification techniques to delineate wild oyster habitats and quantify their area and distribution (Espriella et al., 2020; Espriella & Lecours, 2022; Ridge et al., 2020). Windle et al. (2019) assessed reef area and morphology by comparing RTK-GPS elevation surveys to different UAS aircraft imagery and found minimal differences between the methods, suggesting that UAS is a useful tool for intertidal oyster reef monitoring. Other ground-based sensors, such as terrestrial laser scanners (TLS), have been used to compare models created using UAS SfM (Ridge et al., 2023). Their results showed that UAS SfM structural metrics assessed were consistent with the TLS results, with a UAS workflow being more efficient for data processing and analysis (Ridge et al., 2023). A study by Windle et al. (2022) leveraged spectral characteristics of orthomosaics using unsupervised classification combined with surface complexity to estimate oyster density. However, this study had various limitations such as the challenge of obtaining the optimal conditions to capture accurate spectral characteristics of oyster reefs (Windle et al., 2022). Hoffmann et al. (2023) also showed how UAS SfM geospatial products can be classified using random forest algorithms to assess oyster reef volumetric growth changes, although the authors had challenges with capturing small-scale changes. Lastly, UAS with multi-spectral sensors have been implemented to detect oyster-farming tables and mesh bags at different altitudes, showing promise for mapping oyster aquaculture (Román et al., 2023). Despite advancements in the application of UAS in this field, challenges remain in obtaining detailed spatial and temporal assessments, specifically for intertidal oyster reefs. To our knowledge, no previous studies have developed a reef metric using oyster cluster features (i.e., groups of oysters that have settled on top of one another and form a distinct clump) derived only from SfM to

evaluate spatial and temporal dynamics of oyster populations.

In this study, we combine UAS imagery and field survey data to quantitatively explore the application of UAS as a monitoring tool for intertidal oyster reefs within and adjacent to Apalachicola Bay, Florida. Apalachicola Bay is an interesting case study for this work given its long history as an important area for oyster harvest, recent collapses of oyster populations and subsequent closures to oyster harvesting in the Bay and the presence of extensive intertidal reefs in addition to subtidal reefs (Grizzle et al., 2018). The specific objectives of our study are to examine how (1) geospatial products developed from UAS imagery can be utilized to digitally recreate intertidal oyster reef features (i.e., oyster clusters), (2) cluster sampling data can be extrapolated to UAS geospatial data products and (3) these methods can be applied to assess temporal changes or spatial variation across the study area. This research may facilitate a rapid, low-cost, labor-saving and spatially comprehensive tool for coastal managers to utilize for intertidal oyster reef condition monitoring.

Materials and Methods

Study area

The Apalachicola Bay, on the northern Florida coast of the Gulf of Mexico, is an estuary fed by the Apalachicola-Chattahoochee-Flint river system and spans about 62 000 hectares with depths between 2 and 3 m at mean low tide (Livingston, 1984; Fig. 1). This highly productive estuary once provided up to 90% of Florida's oysters and 10% of the USA market supply (MacKenzie et al., 1997). From 2006 to 2013, the region was subject to a series of severe droughts (Camp et al., 2015), which potentially increased parasites, predators and disease, increasing oyster juvenile mortality (Camp et al., 2015). A reef replenishment (re-shelling) program ended and harvest continued with limited restrictions on increasingly depleted reefs, resulting in declining areas for larval settlement (Camp et al., 2015; Pine III et al., 2015). These factors contributed to a population collapse in 2012 (Camp et al., 2015), with the fishery officially declared a Federal Fisheries Disaster in 2013. Despite this declaration, commercial harvesting continued until December of 2020 when Apalachicola Bay was closed to all harvesting for 5 years by the Florida Fish and Wildlife Conservation Commission. However, this closure did not include locations outside Apalachicola Bay, such as Alligator Harbor, potentially increasing the harvest pressure on those areas.

While subtidal oyster populations in Apalachicola Bay have been extensively monitored and studied since the

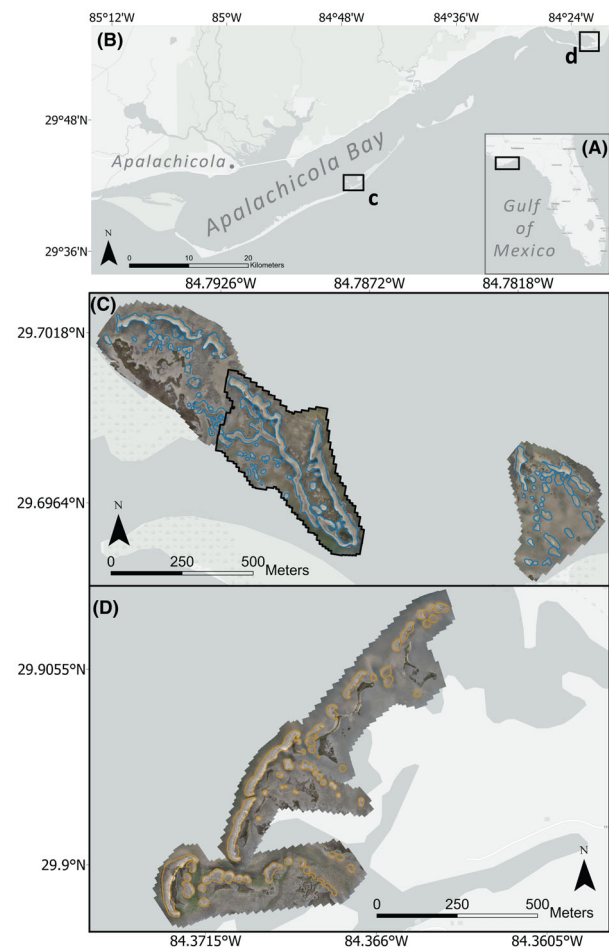


Figure 1. (A) Map of the Apalachicola Bay region in (B) northern Florida, with insets of (C) East Cove (EC) located on St. George Island, showing oyster reef boundaries in blue, and (D) Alligator Harbor (AH), east of Apalachicola Bay, showing oyster reef boundaries in orange.

collapse, intertidal populations have not been included in agency monitoring programs. However, intertidal reefs are an important component of the ecosystem (Peterson et al., 2003; Wiberg et al., 2019), and ideally monitoring programs should include intertidal reefs located in areas that are open and closed to commercial harvesting to help assess the effects of increased harvest pressure on intertidal oyster populations. Intertidal oyster reefs cover about 94 hectares of the bay based on data collected in 2013 and 2015 (Grizzle et al., 2018), including Indian Lagoon in the west—areas near Little St. George Island, St. George Island and Apalachicola (Grizzle et al., 2018)—and reefs near Carrabelle River and Alligator Harbor to the east, both outside the Apalachicola Bay system bounds. The tides range from semidiurnal in the east to diurnal in the west of the bay (Huang et al., 2002). We chose two focal sites for this research, East Cove (EC),

which is closed to harvesting, and Alligator Harbor (AH), which is partially open to harvesting (Fig. 1).

Field data collection

We flew all sections using a DJI Phantom 4 Pro V2 UAS with a 20Mpix RGB (Red-Green-Blue) camera with identical mission settings. Prior to being in the field, we used DJI Ground Station Pro software to create our flight plans, ensuring coverage of the reefs identified by Grizzle et al. (2018). Due to the software's limitation of 99 waypoints per flight plan, we divided larger areas into separate flight plans to maximize coverage and include as many reefs as possible, resulting in dividing AH and EC into three sections each. The flight settings include 75% side and 70% front image overlap at a 40-m altitude. This altitude provided about a 1.5 cm/pixel ground sampling distance. We surveyed EC on 7 December 2021, 4 January 2022 and 23 January 2023, and surveyed AH on 5 January 2022 and 2 March 2022. We placed ground control points (GCPs)—black and white 0.6 by 0.6 m targets used to increase accuracy of UAS geospatial products—on the reefs before each flight. A minimum of three GCPs is required to produce photogrammetric products (Smith et al., 2016), but at least 10 evenly spread GCPs can produce high-quality results (Agisoft Metashape Professional, 2020). Therefore, we placed between nine and 12 GCPs within each flight mission boundary. We surveyed the GCPs using a Trimble Catalyst V1 and V2 antenna with 1- to 2-cm vertical accuracy via the Trimble Corrections Hub.

We revisited two flight sections for cluster sampling and ground truthing. At AH, we collected 14 clusters at random on 22 November 2022, but did not conduct ground truthing because of logistical constraints. At EC on 23 January 2023, we conducted ground truthing surveying 35 random points *in situ* by recording the location (using the Trimble unit) and presence or absence of clusters in order to assess the accuracy of clusters identified with the UAS imagery. We also collected 13 oyster clusters at random at EC. Collected clusters from both sites were processed in the lab by measuring the overall cluster height, width and length (Figure S1). We also deconstructed the clusters to count boxes (dead oysters with articulated shells), single shells from dead oysters and live oysters (Figure S1; Table S1). The respective heights were recorded for each individual live oyster, measured from the umbo to the distal margin of the shell (Baggett, 2014; Figure S1). Additionally, in March of 2023, we surveyed 30 *in situ* quadrats (each 625 cm²) in areas without clusters at EC. Within these non-cluster quadrats, we counted and measured the heights of oyster boxes and live oysters encountered (Table S2).

Data processing

We processed the UAS imagery and GPS data in Agisoft Metashape software version 1.8.4 (Agisoft Metashape Professional, 2022), using structure from motion (SfM) photogrammetry techniques, following the USGS protocol to process coastal imagery (Over et al., 2021). The workflow involved the following steps: align photos, manually identify GCPs, optimize cameras (using GCPs only), filter sparse cloud points and build a dense cloud. This yielded a DEM and an orthomosaic (Over et al., 2021). Other steps added to this workflow include converting the imagery coordinate system to match the GPS data (NAD1983 (2011) UTM 16 zone NAVD 88), assessing quality of the imagery, classifying any extraneous dense cloud points as noise and creating a DEM from the non-noise points. The resolution of the orthomosaics was 1 cm/pixel, and the DEMs were 2 cm/pixel. The DEM and orthomosaic from each site were exported with the projected coordinate system: NAD1983 (2011) UTM 16 zone and NAVD88 vertical datum, in meters.

We further processed the orthomosaics and DEMs in ArcGIS Pro to create reef boundaries and extract clusters. We manually created reef boundaries by using the orthomosaics and DEMs to delineate between shell and non-shell areas (Fig. 1). This manual delineation was done using visual characteristics of brighter, light colors to distinguish shell substrate and darker colors for mud substrate. We clipped the DEMs using the reef boundaries in ArcGIS Pro. Because oysters settle on top of each other, they create clusters that are a prominent feature in DEMs (Fig. 2; Figure S1). We extracted these cluster features by calculating the mean curvature of the clipped DEM surface using the ArcGIS Pro 'Surface Parameter' tool with the mean curvature parameter. To reduce noise, we increased the neighborhood distance to a scale that is 10 times larger than the input cell size. The mean curvature tool is typically used to indicate areas of maximum denudation or accumulation, by calculating how a surface deviates from flatness at each point (Minár et al., 2020). The resulting mean curvature surface was reclassified and then converted to a vector file in ArcGIS Pro, providing the area and location of each cluster. The smallest cluster from the field cluster sampling measured 66 cm², and the largest measured 736 cm²; therefore, we used 50 and 800 cm² as the lower and upper cluster size limits for inclusion in the vector file containing the extracted clusters, derived from the mean curvature of the DEM. This approach helps reduce uncertainty associated with the counts of live oysters in clusters that were much smaller or larger than the sampled clusters. Additionally, other polygons that were not oyster reef features, such as kayaks or salt marsh, were also removed from the vector file.

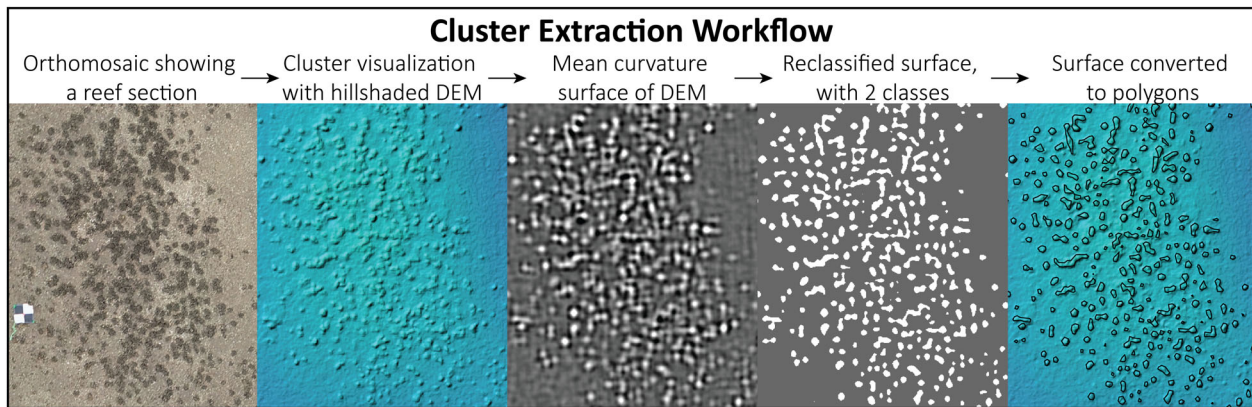


Figure 2. Example of the cluster extraction process at East Cove (EC) Section 1 on St. George Island, Florida utilizing GIS software.

Statistical analysis

We conducted statistical analyses using R (version 4.3.1) and RStudio (version 2023.06.2). To compare the number of live oysters in non-cluster and cluster data, we used a Wilcoxon test. Throughout our analyses, we used this non-parametric test due to the non-normally distributed and zero-inflated nature of the datasets. To estimate the overall number of oysters in clusters, we performed a linear regression analysis to model the relationship between live oyster count (the response variable) and cluster size (the predictor variable) for the sampled clusters collected at AH and EC, using both separate and combined models. We also performed a Wilcoxon test to confirm similar oyster size distributions within the clusters across these two sites to verify that size differences would not confound the cluster size and oyster count relationship. Using the combined regression model and the standard error estimates of the model coefficients, we estimated the number of live oysters for the extracted clusters in the vector file, with the respective polygon sizes derived from the mean curvature of the DEM. This was done using the ‘predict’ function within the ‘stats’ base package in R. For our spatial analysis, we predicted live oyster counts for all clusters extracted from EC and AH areas. To compensate for the difference in reef number and area between both sites, we divided the number of live oysters by reef area to produce a spatial density value for each location. We compared extracted cluster sizes and oyster densities for each reef in AH and EC using Wilcoxon tests. We conducted a temporal analysis for one section of EC that had repeated monitoring in 2022 and 2023. Using the same model, we predicted live oyster counts for each year. We compared the extracted cluster sizes between years using histograms and a Wilcoxon test. We also compared the densities for each reef between both years using a Wilcoxon test.

For accuracy assessment of our ground-truthing data compared to the geospatial cluster extractions, we employed a confusion matrix, treating the true ground-truthing data as actual and the geospatial clusters data as predicted (Table S3). The accuracy was calculated as the sum of true positives and true negatives divided by the total sum of all the confusion matrix values (Table S3).

Results

We mapped 43.5 hectares of oyster reef, tidal flat, seagrass and salt marsh in the orthomosaics and DEMs in 2022 (Fig. 1), which included 82 reefs covering about 89 922 m² at EC (Table 1). The reef sizes in this section were variable, ranging from 44 to 21 771 m². Within the EC reefs, there were 94 831 oyster cluster polygons for a total area of 2642 m², or 2.9% of reef area. We mapped 33.4 hectares of oyster reef, tidal flat, seagrass and salt marsh in the orthomosaics and DEMs at AH in January 2022 (Fig. 1D), which included a total of 56 reefs covering 48 460 m² (Table 1). The reef sizes in this section ranged from 48 to 6650 m². Within the AH reefs, there were 41 101 oyster cluster polygons for a total area of 1147 m² or 2.4% of the reef area.

Ground truthing and cluster sampling

At section 1 of EC (Fig. 1C), we cross-referenced the ground-truthing field data of cluster presence and absence with the final dataset containing cluster extractions. The confusion matrix revealed a 97.14% accuracy in correctly identifying the clusters (Table S3). We conducted a comparative analysis of oyster cluster ($n = 13$) and non-cluster ($n = 30$) areas at EC. In non-cluster areas, the average live oyster density was 12 ± 5 oysters per m², while in cluster areas, it was orders of magnitude higher at 1209 ± 184 oysters per m²—a highly significant difference in live

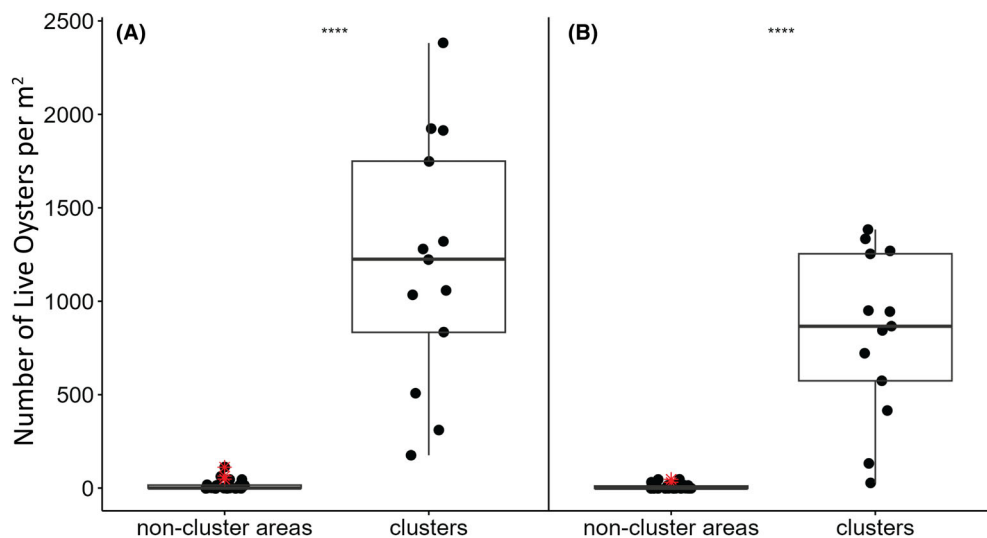
Table 1. Summary of spatial analysis for Alligator Harbor (AH) and East Cove (EC) and summary of temporal analysis for EC between 2022 and 2023.

	No. of reefs	Area of reefs (m ²)	No. of clusters	Area of clusters (m ²)	Predicted number of live oysters (including spat)	Predicted number of live oysters (excluding spat)	Live oysters per m ² (including spat)	Live oysters per m ² (excluding spat)
Spatial analysis								
Alligator Harbor	56	48 460	41 101	1147	1 567 009 ± 127 525	990 491 ± 79 382	32.4	20.4
East Cove	82	89 922	94 831	2642	3 611 167 ± 293 881	2 282 584 ± 182 934	40.2	25.4
Temporal analysis								
East Cove- 2022	25	46 958	61 222	1785	2 439 609 ± 198 538	1 542 053 ± 123 588	52	32.8
East Cove- 2023	25	46 958	59 326	1711	2 338 241 ± 190 289	1 477 979 ± 118 451	49.8	31.5

oyster densities supporting our approach of using clusters as proxies for oyster presence (Fig. 3; Wilcoxon rank sum test; $P < 0.0001$). We also excluded oysters smaller than 2.5 cm from both datasets to account for high rates of juvenile (spat) mortality that may not contribute long term to the oyster population. Without spat included, the live oyster density in non-cluster areas was 7 ± 3 oysters per m², while in cluster areas, live oyster density was 825 ± 122 oysters per m², also a large and statistically significant difference (Fig. 3B; $P < 0.0001$).

We fit a linear regression model to explore the relationship of cluster size with number of live oysters. First, we analyzed the oyster size frequency distribution of AH and EC and did not find a significant difference in the distribution of oyster sizes between AH and EC (Figure S2A, Wilcoxon test; $P > 0.05$). Additionally, separate

regressions of cluster size predicting live oyster count showed similar positive relationships (Figure S2B–E). Therefore, we combined the clusters collected from AH and EC to increase the sample size (Fig. 4). These clusters ranged from 66 to 736 cm² and the number of live oysters per cluster ranged from 0 to 131. The regression model showed, on average, an increase of 0.137 live oysters for a 1 cm² increase in cluster size (Fig. 4A; $R^2 = 0.853$; $P < 0.0001$). To exclude recent spat settlement that may not contribute long term to the cluster given high rates of spat mortality, oysters smaller than 2.5 cm were also removed from the dataset. After excluding spat, the number of live oysters ranged from 0 to 70. The regression model showed, on average, an increase of 0.086 live oysters for a 1 cm² increase in cluster size (Fig. 4B, $R^2 = 0.857$; $P < 0.0001$).

**Figure 3.** Comparison of live oyster densities between cluster areas and non-cluster areas (A) including live oysters smaller than 2.5 cm and (B) excluding live oysters smaller than 2.5 cm. Black asterisks indicate the statistical significance between groups conducted using a Wilcoxon test. Red asterisks indicate outliers.

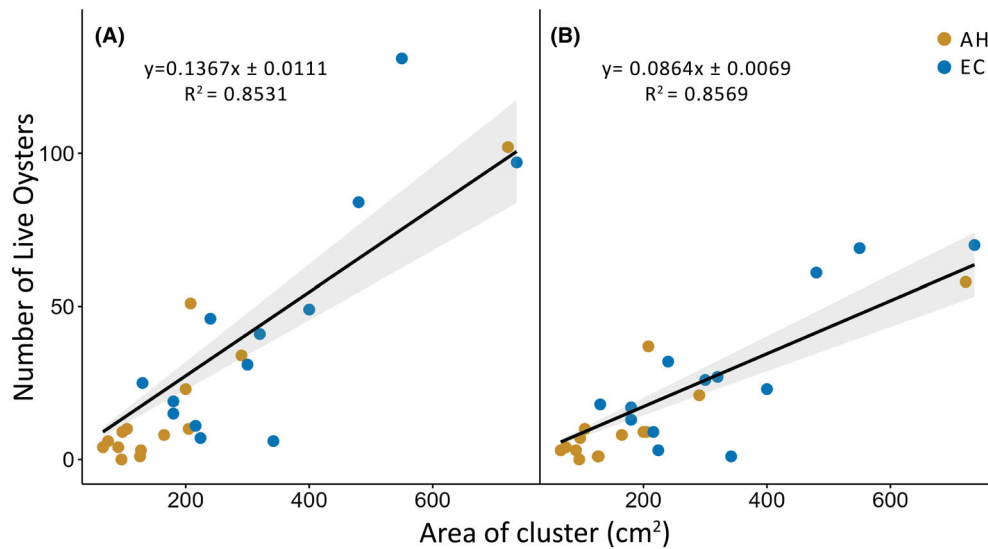


Figure 4. Linear regression models of live oyster count and area of cluster for Alligator Harbor (AH) and East Cove (EC), $n = 27$, (A) including oysters smaller than 2.5 cm and (B) excluding oysters smaller than 2.5 cm. The black line represents the regression line, and the gray shading is the 95% confidence interval.

Spatial analysis

We estimated the total number of live oysters at AH and EC using regression predictions to compare these two distinct locations (Table 1; Fig. 1). In 2022, we estimated more live oysters at EC than at AH, whether spat was included or excluded (Table 1). We compared the cluster sizes between AH and EC, revealing a statistical difference between sites (Figure S3A, $P < 0.0001$). Whether or not spat were included, EC had a higher average density of live oysters than AH (e.g., 40.2 vs. 32.4 oysters/m² including spat; Table 1). Live oyster density at both sites varied across the reefs (Fig. 5). A Wilcoxon test revealed a statistical difference in live oyster densities per reef between sites (Figure S3B; $P < 0.0001$).

Temporal analysis

In 2023, we mapped EC section 1 within the same boundaries as in 2022 for a direct comparison of 25 reefs (Fig. 1C). The reef sizes in this subsection ranged from 57 to 21 771 m². The number of clusters decreased from 2022 to 2023 by 1896 clusters (Table 1), which resulted in a loss of 74 m² (or 4.14%) in total cluster area. The loss of clusters in 2023 was not uniform across cluster sizes; most of the losses were of smaller clusters, between 0.005 and 0.015 m², and larger clusters, between 0.025 and 0.08 m², and there were more intermediate-sized clusters, 0.015–0.025 m², in 2023 (Figure S4). We compared the cluster sizes between 2022 and 2023, revealing a slight statistical difference between years (Figure S5A, $P < 0.01$).

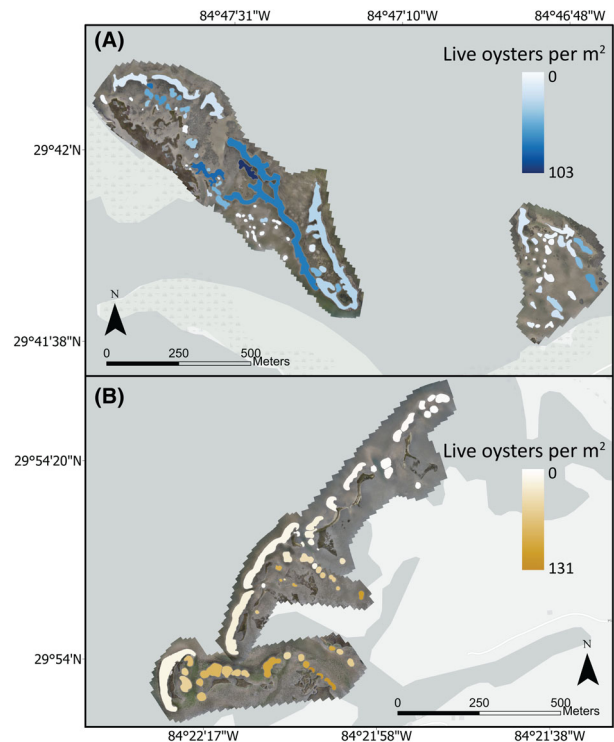


Figure 5. Density of live oysters per reef at (A) East Cove (EC) and (B) Alligator Harbor (AH).

The regression models of cluster size predicting live oyster counts were applied to all clusters within this section to compare temporal changes in live oysters between

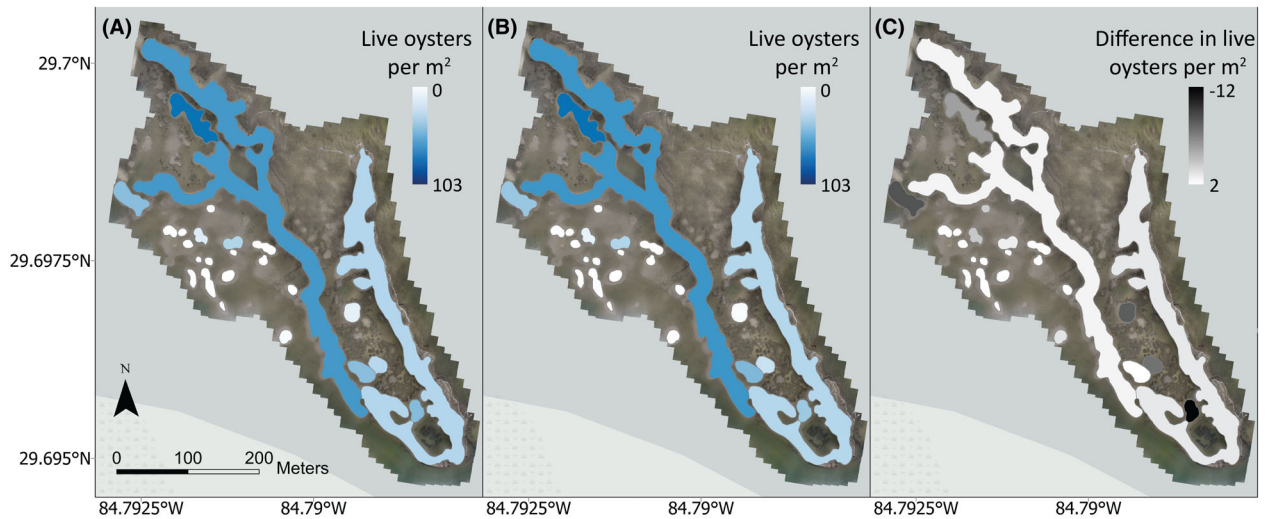


Figure 6. Oyster density maps for East Cove (EC) section 1 in (A) 2022 and (B) 2023; (C) Map depicting the difference in reef densities between the 2 years.

the years (Table 1; Fig. 6). There was a decrease in live oysters from 2022 to 2023, whether spat was included or excluded (Table 1). However, the standard errors of predicted live oysters between both years fall within the range of the observed difference (Table 1). We also calculated the live oyster densities per reef, showing a slight decrease from 2022 to 2023 (e.g., 52 vs. 49.8 oysters/m² including spat; Table 1). However, a Wilcoxon test revealed no statistical difference in live oyster densities per reef between years (Figure S5B, $P > 0.05$). There were relatively similar spatial patterns of oyster density across the reefs between both years (Fig. 6).

Discussion

We demonstrate the successful application and interpretation of UAS SfM products and field sampling to establish a framework for spatial and temporal monitoring of intertidal oyster reef condition. Field sampling revealed that cluster areas extracted from orthomosaics and DEMs have 100 times greater average live oyster abundance than non-cluster areas, verifying that we are able to use our UAS methods to identify the majority of intertidal oysters. We also found a predictable relationship between cluster size and number of live oysters, validating our use of the sizes of cluster features as a proxy for oyster reef condition. Using SfM products consisting of DEMs and orthomosaics, we identified and extracted oyster cluster polygons with their respective sizes and applied a predictive model to estimate the number of live oysters per cluster at two locations. Our findings highlight notable spatial variation in reef condition, with AH exhibiting

nearly 50% lower estimated live oyster counts and lower live oyster density compared to EC. A temporal assessment of one section of EC between 2022 and 2023 revealed a decrease in cluster count, a small percent decrease in total cluster area and a relatively stable oyster density. Despite a slight decrease in live oyster density, the standard errors fall within the range of the observed difference, suggesting that the decrease may be due to random variations within the data rather than a significant ecological change.

The observed spatial and temporal differences in oyster abundance on the reefs in these two sites may be attributed to various factors. For instance, the spatial differences between AH and EC may be influenced by their current regulation status. AH is outside the bounds of Apalachicola Bay and most reefs on the northern side of AH are in areas approved for harvesting (Rulemaking Authority Art. IV, 2021). EC is located on the bay side of St. George Island, within the Apalachicola Bay bounds where oyster harvesting is currently prohibited (Rulemaking Authority Art. IV, 2021). The observed spatial differences in oyster density and live oyster abundance between the northern and southern parts of AH and from AH to EC (Fig. 5) could be at least partially attributed to differences in harvest pressure. Currently, the harvesting limit in open areas is 20 bags of oysters per person or vessel per day (Rulemaking Authority Art. IV, 2021). It is also possible that AH has historically exhibited lower densities due to other local-scale factors not related to fishing pressure. These factors include salinity, oxygen availability, the duration of inundation, predation and competition (Dame, 2012; Luckenbach et al., 1999). Further, oyster

densities across both sites and years tend to be higher on the largest reefs, while smaller reefs exhibit lower densities (Fig. 5), which may indicate the importance of these larger reefs for oyster population maintenance (Eggleston, 1999). Finally, the arrangement of reefs relative to hydrodynamic forces may also be important and could actually be driving the pattern of higher densities on larger reefs. Specifically, if the larger reefs in the EC area experience optimal hydrodynamic conditions, being oriented perpendicular to the direction of tidal flow, this would facilitate waste removal and increase the flow of particles and oxygen (Colden et al., 2016), allowing these areas to support higher oyster densities.

While this study presents a promising methodology for intertidal oyster reef monitoring, there are some important limitations with the methodology and the data collected in this study. For instance, this method can be applied to a new region; however, cluster sampling should be conducted in each new region to account for potential differences in the oyster cluster morphology. Differences in size distribution of the oysters may influence composition and characteristics of oyster reef clusters between regions (Byers et al., 2015). Therefore, oyster size distribution should be assessed before merging and applying regression models. Further, this study relies on cluster sampling to predict live oyster estimates from geospatial data but does not use information on the relationship between spat quantity and cluster size. Given the importance of recruitment rates for sustaining oyster populations (Coen & Luckenbach, 2000), it is useful to monitor spat recruitment rates. Therefore, combining this method that assesses large areas with a more focused on the ground sampling is recommended (Coen & Luckenbach, 2000). Another consideration is the narrow windows of reef exposure co-occurring during daylight hours and low tides, which mainly occurred during the winter in our study region. Thus, this approach may be unable to capture shorter term dynamics, such as seasonal variations in reef condition. Finally, a main data limitation in this study is the small sample size of oyster clusters collected ($n = 27$). A more extensive dataset, with a broader range of cluster sizes, would have made our regression models more robust. Additionally, the lower and upper limits of cluster sizes extracted from the geospatial data were based on the smallest and largest clusters sampled, which was a necessary practical approach. However, collecting even smaller and larger clusters might yield different live oyster density numbers, potentially affecting the final data outputs and improving the precision of our geospatial analysis. Despite these limitations, this method provides a generally reliable monitoring approach that could be particularly valuable for locations that are difficult to access, allowing for more consistent and recurrent monitoring.

UAS offers several advantages over other methods that can be used for oyster monitoring. UAS can sample a significantly larger area in a relatively short amount of time, improving efficiency and data collection capabilities. They are also a cost-effective option with flexibility to customize various settings, including altitude and image overlap to suit specific research needs. Additionally, when combining the high overlapping imagery with SfM techniques, key features can be extracted. Looking forward, combining UAS with other existing and emerging technologies could further improve monitoring. In particular, LiDAR and multispectral sensors have shown promising results for intertidal oyster reef monitoring (Chand & Bollard, 2021; Espriella et al., 2023), providing precise topographical data with LiDAR and useful spectral information from multispectral imaging. For instance, Espriella et al. (2023) found that using UAS with LiDAR sensors to assess surface complexity metrics effectively predicted intertidal oyster reef condition. Additionally, multispectral sensors have been shown to improve wild oyster reef detection (Chand & Bollard, 2021). By integrating these technologies with our method, researchers can enhance cluster identification and extrapolation to determine cluster size and number of live oysters, with a higher degree of accuracy. These spatial distribution measurements can then be coupled with other physical or biological factors to understand differences across or within sites (Byers et al., 2015). For instance, salinity, temperature, flow patterns, inundation duration and depth of inundation can provide insights into potential factors driving differences in population densities (Colden et al., 2016; Luckenbach et al., 1999). Additionally, biotic interactions, such as the presence of predators, should also be considered, as they can also influence oyster densities (Bartol et al., 1999; Grabowski, 2004).

Beyond the immediate impact of direct anthropogenic activities such as harvesting, oyster reefs face other threats, both natural and anthropogenic (Beck et al., 2011; Kennish, 2002). Climate change will increase a range of challenges, including drought, hurricanes, sea-level rise and shifts in temperature that can affect oyster populations (Camp et al., 2015; Solomon et al., 2014). In the face of these threats, UAS technology is valuable for the rapid assessment of damage and the monitoring of recovery efforts. This framework can serve as a useful tool in conservation and restoration to make informed decisions to protect and rehabilitate coastal ecosystems like oyster reefs.

Acknowledgments

We gratefully acknowledge the support received from the Triumph Gulf Coast Inc. funding agency for the

Apalachicola Bay System Initiative (grant no. 69), which funded and facilitated this research. This work was completed under permit SAL-22-2197-SR. Logistic support to visit East Cove and Alligator Harbor near Apalachicola Bay was provided by the Florida State University Coastal and Marine Laboratory. We thank the ABSI team members for their extensive assistance in both fieldwork and laboratory activities throughout the years. We would also like to thank the members of the Rasster lab for their constructive feedback at various stages of the project.

References

- Agisoft Metashape Professional. (2020) Agisoft. LLC (Professional Edition), St. Petersburg, Russia. Available from: https://www.agisoft.com/pdf/metashape-pro_1_6_en.pdf
- Agisoft Metashape Professional. (2022) Agisoft. LLC (Professional Edition), St. Petersburg, Russia.
- Baggett, L.P., Powers, S.P., Brumbaugh, R., Coen, L.D., DeAngelis, B., Greene, J. et al. (2014) *Oyster habitat restoration monitoring and assessment handbook*. Arlington, VA, USA: The Nature Conservancy, p. 96.
- Baggett, L.P., Powers, S.P., Brumbaugh, R.D., Coen, L.D., DeAngelis, B.M., Greene, J.K. et al. (2015) Guidelines for evaluating performance of oyster habitat restoration: evaluating performance of oyster restoration. *Restoration Ecology*, **23**(6), 737–745. Available from: <https://doi.org/10.1111/rec.12262>
- Bahr, L.M. & Lanier, W.P. (1981) *The ecology of intertidal oyster reefs of the South Atlantic Coast: a community profile*. OBS-81/15. Washington DC: U.S. Fish and Wildlife Service, Office of Biological Services FWS, p. 105.
- Bartol, I.K., Mann, R. & Luckenbach, M. (1999) Growth and mortality of oysters (*Crassostrea virginica*) on constructed intertidal reefs: effects of tidal height and substrate level. *Journal of Experimental Marine Biology and Ecology*, **237**(2), 157–184. Available from: [https://doi.org/10.1016/S0022-0981\(98\)00175-0](https://doi.org/10.1016/S0022-0981(98)00175-0)
- Beck, M.W., Brumbaugh, R.D., Airoidi, L., Carranza, A., Coen, L.D., Crawford, C. et al. (2011) Oyster reefs at risk and recommendations for conservation, restoration, and management. *Bioscience*, **61**(2), 107–116. Available from: <https://doi.org/10.1525/bio.2011.61.2.5>
- Benson, G.W., Donnelly, M.J., Sacks, P.E. & Walters, L.J. (2023) Documenting loss and fragmentation of intertidal oyster (*Crassostrea virginica*) reefs in a subtropical estuary. *Environments*, **10**(8), 133. Available from: <https://doi.org/10.3390/environments10080133>
- Byers, J.E., Grabowski, J.H., Piehler, M.F., Hughes, A.R., Weiskel, H.W., Malek, J.C. et al. (2015) Geographic variation in intertidal oyster reef properties and the influence of tidal prism: biogeography of intertidal oyster reefs. *Limnology and Oceanography*, **60**(3), 1051–1063. Available from: <https://doi.org/10.1002/lno.10073>
- Camp, E.V., Pine, W.E., III, Havens, K., Kane, A.S., Walters, C.J., Irani, T. et al. (2015) Collapse of a historic oyster fishery: diagnosing causes and identifying paths toward increased resilience. *Ecology and Society*, **20**(3), art45. Available from: <https://doi.org/10.5751/ES-07821-200345>
- Casella, E., Collin, A., Harris, D., Ferse, S., Bejarano, S., Parravicini, V. et al. (2017) Mapping coral reefs using consumer-grade drones and structure from motion photogrammetry techniques. *Coral Reefs*, **36**(1), 269–275. Available from: <https://doi.org/10.1007/s00338-016-1522-0>
- Chand, S. & Bollard, B. (2021) Multispectral low altitude remote sensing of wild oyster reefs. *Global Ecology and Conservation*, **30**, e01810. Available from: <https://doi.org/10.1016/j.gecco.2021.e01810>
- Coen, L.D. & Luckenbach, M.W. (2000) Developing success criteria and goals for evaluating oyster reef restoration: ecological function or resource exploitation? *Ecological Engineering*, **15**(3–4), 323–343. Available from: [https://doi.org/10.1016/S0925-8574\(00\)00084-7](https://doi.org/10.1016/S0925-8574(00)00084-7)
- Coen, L.D., Luckenbach, M.W. & Breitburg, D.L. (1999) The role of oyster reefs as essential fish habitat: a review of current knowledge and some new perspectives. American Fisheries Society Symposium.
- Colden, A.M., Fall, K.A., Cartwright, G.M. & Friedrichs, C.T. (2016) Sediment suspension and deposition across restored oyster reefs of varying orientation to flow: implications for restoration. *Estuaries and Coasts*, **39**(5), 1435–1448. Available from: <https://doi.org/10.1007/s12237-016-0096-y>
- Dame, R.F. (Ed.). (2012) *Ecology of marine bivalves: an ecosystem approach*, 2nd edition. Boca Raton: Taylor & Francis.
- Dance, M.A., Rooker, J.R., Kline, R.J., Quigg, A., Stunz, G.R., Wells, R.J.D. et al. (2021) Importance of low-relief nursery habitat for reef fishes. *Ecosphere*, **12**(6), e03542. Available from: <https://doi.org/10.1002/ecs2.3542>
- Drexler, M., Parker, M.L., Geiger, S.P., Arnold, W.S. & Hallock, P. (2014) Biological assessment of eastern oysters (*Crassostrea virginica*) inhabiting reef, mangrove, seawall, and restoration substrates. *Estuaries and Coasts*, **37**(4), 962–972. Available from: <https://doi.org/10.1007/s12237-013-9727-8>
- Dronova, I., Kislik, C., Dinh, Z. & Kelly, M. (2021) A review of unoccupied aerial vehicle use in wetland applications: emerging opportunities in approach, technology, and data. *Drones*, **5**(2), 29. Available from: <https://doi.org/10.3390/drones5020045>
- Eggleston, D.B. (1999) *Application of landscape ecological principles to oyster reef habitat restoration*. Gloucester Point, VA: Virginia Institute of Marine Science Press, pp. 213–227.
- Espriella, M.C. & Lecours, V. (2022) Optimizing the scale of observation for intertidal habitat classification through

- multiscale analysis. *Drones*, **6**(6), 140. Available from: <https://doi.org/10.3390/drones6060140>
- Espriella, M.C., Lecours, V., C. Frederick, P., V. Camp, E. & Wilkinson, B. (2020) Quantifying intertidal habitat relative coverage in a Florida estuary using UAS imagery and GEOBIA. *Remote Sensing*, **12**(4), 677. Available from: <https://doi.org/10.3390/rs12040677>
- Espriella, M.C., Lecours, V., Camp, E.V., Andrew Lassiter, H., Wilkinson, B., Frederick, P.C. et al. (2023) Drone lidar-derived surface complexity metrics as indicators of intertidal oyster reef condition. *Ecological Indicators*, **150**, 110190. Available from: <https://doi.org/10.1016/j.ecolind.2023.110190>
- Garvis, S., Donnelly, M., Hernandez, E., Walters, L., Weishampel, J. & Brockmeyer, R. (2020) Remote sensing of live and dead intertidal oyster reefs using aerial photo interpretation in Northeast Florida. *Journal of Coastal Conservation*, **24**(1), 14. Available from: <https://doi.org/10.1007/s11852-020-00728-w>
- Garvis, S.K., Sacks, P.E. & Walters, L.J. (2015) Formation, movement, and restoration of dead intertidal oyster reefs in Canaveral National Seashore and mosquito lagoon, Florida. *Journal of Shellfish Research*, **34**(2), 251–258. Available from: <https://doi.org/10.2983/035.034.0206>
- Grabowski, J.H. (2004) Habitat complexity disrupts predator–prey interactions but not the trophic cascade on oyster reefs. *Ecology*, **85**(4), 995–1004. Available from: <https://doi.org/10.1890/03-0067>
- Gray, P., Ridge, J.T., Poulin, S.K., Seymour, A.C., Schwantes, A.M., Swenson, J.J. et al. (2018) Integrating drone imagery into high resolution satellite remote sensing assessments of estuarine environments. *Remote Sensing*, **10**(8), 1257. Available from: <https://doi.org/10.3390/rs10081257>
- Grizzle, R., Ward, K., Geselbracht, L. & Birch, A. (2018) Distribution and condition of intertidal eastern oyster (*Crassostrea virginica*) reefs in Apalachicola Bay Florida based on high-resolution satellite imagery. *Journal of Shellfish Research*, **37**(5), 1027. Available from: <https://doi.org/10.2983/035.037.0514>
- Hoffmann, T.K., Pfennings, K., Hitzegrad, J., Brohmann, L., Welzel, M., Paul, M. et al. (2023) Low-cost UAV monitoring: insights into seasonal volumetric changes of an oyster reef in the German Wadden Sea. *Frontiers in Marine Science*, **10**, 1245926. Available from: <https://doi.org/10.3389/fmars.2023.1245926>
- Huang, W., Jones, W.K. & Wu, T.S. (2002) Modelling wind effects on subtidal salinity in Apalachicola Bay, Florida. *Estuarine, Coastal and Shelf Science*, **55**(1), 33–46. Available from: <https://doi.org/10.1006/ecss.2001.0881>
- Joyce, K.E., Duce, S., Leahy, S.M., Leon, J. & Maier, S.W. (2019) Principles and practice of acquiring drone-based image data in marine environments. *Marine and Freshwater Research*, **70**(7), 952–963. Available from: <https://doi.org/10.1071/MF17380>
- Kalacska, M., Chmura, G.L., Lucanus, O., Bérubé, D. & Arroyo-Mora, J.P. (2017) Structure from motion will revolutionize analyses of tidal wetland landscapes. *Remote Sensing of Environment*, **199**, 14–24. Available from: <https://doi.org/10.1016/j.rse.2017.06.023>
- Kennish, M.J. (2002) Environmental threats and environmental future of estuaries. *Environmental Conservation*, **29**(1), 78–107. Available from: <https://doi.org/10.1017/S0376892902000061>
- Klemas, V.V. (2015) Coastal and environmental remote sensing from unmanned aerial vehicles: an overview. *Journal of Coastal Research*, **315**, 1260–1267. Available from: <https://doi.org/10.2112/JCOASTRES-D-15-00005.1>
- Lenihan, H.S., Micheli, F., Shelton, S.W. & Peterson, C.H. (1999) The influence of multiple environmental stressors on susceptibility to parasites: an experimental determination with oysters. *Limnology and Oceanography*, **44**(3part2), 910–924. Available from: https://doi.org/10.4319/lo.1999.44.3_part_2.0910
- Lenihan, H.S. & Peterson, C.H. (1998) How habitat degradation through fishery disturbance enhances impacts of hypoxia on oyster reefs. *Ecological Applications*, **8**(1), 128–140. Available from: [https://doi.org/10.1890/1051-0761\(1998\)008\[0128:HHDTFD\]2.0.CO;2](https://doi.org/10.1890/1051-0761(1998)008[0128:HHDTFD]2.0.CO;2)
- Leon, J.X., Roelfsema, C.M., Saunders, M.I. & Phinn, S.R. (2015) Measuring coral reef terrain roughness using “structure-from-motion” close-range photogrammetry. *Geomorphology*, **242**, 21–28. Available from: <https://doi.org/10.1016/j.geomorph.2015.01.030>
- Livingston, R.J. (1984) *The ecology of the Apalachicola Bay system: an estuarine profile*. Washington, D.C.: The Service. Available from: <https://doi.org/10.5962/bhl.title.4039>
- Luckenbach, M.W., Mann, R.L. & Wesson, J.A. (1999) Oyster reef habitat restoration: a synopsis and synthesis of approaches. Proceedings from the symposium, Williamsburg, Virginia, April 1995 <https://doi.org/10.21220/V5NK51>
- MacKenzie, C.L., Burrell, V.G., Jr., Rosenfield, A. & Hobart, W.L. (1997) *The history, present condition, and future of the molluscan fisheries of north and Central America and Europe. Volume 1: Atlantic and Gulf coasts*. 127. Seattle, WA, USA: NOAA U.S. Department of Commerce, p. 234. Available from: <https://repository.library.noaa.gov/view/noaa/3011>
- Meyer, D.L. & Townsend, E.C. (2000) Faunal utilization of created intertidal eastern oyster (*Crassostrea virginica*) reefs in the southeastern United States. *Estuaries*, **23**(1), 34. Available from: <https://doi.org/10.2307/1353223>
- Minár, J., Evans, I.S. & Jenčo, M. (2020) A comprehensive system of definitions of land surface (topographic) curvatures, with implications for their application in geoscience modelling and prediction. *Earth-Science Reviews*, **211**, 103414. Available from: <https://doi.org/10.1016/j.earscirev.2020.103414>
- Over, J.-S.R., Andrew C. Ritchie, Christine J. Kranenburg, Jenna A. Brown, Daniel D. Buscombe, Tom Noble,

- Christopher R. Sherwood, Jonathan A. Warrick, and Phillippe A. Wernette (2021) Processing coastal imagery with Agisoft Metashape professional edition, version 1.6—structure from motion workflow documentation. Open-file report 2021–1039. U.S. Geological Survey, p. 46. Available from: <https://pubs.usgs.gov/of/2021/1039/ofr20211039.pdf>.
- Peterson, C., Grabowski, J. & Powers, S. (2003) Estimated enhancement of fish production resulting from restoring oyster reef habitat: quantitative valuation. *Marine Ecology Progress Series*, **264**, 249–264. Available from: <https://doi.org/10.3354/meps264249>
- Piazza, B.P., Banks, P.D. & La Peyre, M.K. (2005) The potential for created oyster Shell reefs as a sustainable shoreline protection strategy in Louisiana. *Restoration Ecology*, **13**(3), 499–506. Available from: <https://doi.org/10.1111/j.1526-100X.2005.00062.x>
- Pine, W.E., III, Walters, C.J., Camp, E.V. & Bouchillon, R. (2015) The curious case of eastern oyster *Crassostrea virginica* stock status in Apalachicola Bay, Florida. *Ecology and Society*, **20**(3), art46. Available from: <https://doi.org/10.5751/ES-07827-200346>
- Ridge, J.T., DiGiacomo, A.E., Rodriguez, A.B., Himmelstein, J.D. & Johnston, D.W. (2023) Comparison of 3D structural metrics on oyster reefs using unoccupied aircraft photogrammetry and terrestrial LiDAR across a tidal elevation gradient. *Remote Sensing in Ecology and Conservation*, **9**(4), 501–511. Available from: <https://doi.org/10.1002/rse2.324>
- Ridge, J.T., Gray, P.C., Windle, A.E. & Johnston, D.W. (2020) Deep learning for coastal resource conservation: automating detection of shellfish reefs. *Remote Sensing in Ecology and Conservation*, **6**(4), 431–440. Available from: <https://doi.org/10.1002/rse2.134>
- Román, A., Prasyad, H., Oiry, S., Davies, B.F.R., Brunier, G. & Barillé, L. (2023) Mapping intertidal oyster farms using unmanned aerial vehicles (UAV) high-resolution multispectral data. *Estuarine, Coastal and Shelf Science*, **291**, 108432. Available from: <https://doi.org/10.1016/j.ecss.2023.108432>
- Rulemaking Authority Art. IV (2021) Apalachicola Bay Oyster Harvesting Restrictions, 68B-27.017. Available from: <https://www.flrules.org/gateway/ruleno.asp?id=68B-27.017>.
- Seavey, J.R., Pine, W.E., III, Frederick, P., Sturmer, L. & Berrigan, M. (2011) Decadal changes in oyster reefs in the big bend of Florida's Gulf Coast. *Ecosphere*, **2**(10), art114. Available from: <https://doi.org/10.1890/ES11-00205.1>
- Smith, M.W., Carrivick, J.L. & Quincey, D.J. (2016) Structure from motion photogrammetry in physical geography. *Progress in Physical Geography*, **40**(2), 247–275. Available from: <https://doi.org/10.1177/0309133315615805>
- Solomon, J.A., Donnelly, M.J. & Walterst, L.J. (2014) Effects of sea level rise on the intertidal oyster *Crassostrea virginica* by field experiments. *Journal of Coastal Research*, **68**, 57–64. Available from: <https://doi.org/10.2112/SI68-008.1>
- Theuerkauf, S.J., Eggleston, D.B., Theuerkauf, K.W. & Puckett, B.J. (2017) Oyster density and demographic rates on natural intertidal reefs and hardened shoreline structures. *Journal of Shellfish Research*, **36**(1), 87–100. Available from: <https://doi.org/10.2983/035.036.0111>
- Ventura, D., Mancini, G., Casoli, E., Pace, D.S., Lasinio, G.J., Belluscio, A. et al. (2022) Seagrass restoration monitoring and shallow-water benthic habitat mapping through a photogrammetry-based protocol. *Journal of Environmental Management*, **304**, 114262. Available from: <https://doi.org/10.1016/j.jenvman.2021.114262>
- Westoby, M.J., Brasington, J., Glasser, N.F., Hambrey, M.J. & Reynolds, J.M. (2012) “Structure-from-motion” photogrammetry: a low-cost, effective tool for geoscience applications. *Geomorphology*, **179**, 300–314. Available from: <https://doi.org/10.1016/j.geomorph.2012.08.021>
- Wiberg, P.L., Taube, S.R., Ferguson, A.E., Kremer, M.R. & Reidenbach, M.A. (2019) Wave attenuation by oyster reefs in shallow coastal bays. *Estuaries and Coasts*, **42**(2), 331–347. Available from: <https://doi.org/10.1007/s12237-018-0463-y>
- Windle, A., Poulin, S., Johnston, D. & Ridge, J. (2019) Rapid and accurate monitoring of intertidal oyster reef habitat using unoccupied aircraft systems and structure from motion. *Remote Sensing*, **11**(20), 2394. Available from: <https://doi.org/10.3390/rs11202394>
- Windle, A.E., Puckett, B., Huebert, K.B., Knorek, Z., Johnston, D.W. & Ridge, J.T. (2022) Estimation of intertidal oyster reef density using spectral and structural characteristics derived from unoccupied aircraft systems and structure from motion photogrammetry. *Remote Sensing*, **14**(9), 16. Available from: <https://doi.org/10.3390/rs14092163>
- zu Ermgassen, P.S.E., Spalding, M.D., Grizzle, R.E. & Brumbaugh, R.D. (2013) Quantifying the loss of a marine ecosystem service: filtration by the eastern oyster in US estuaries. *Estuaries and Coasts*, **36**(1), 36–43. Available from: <https://doi.org/10.1007/s12237-012-9559-y>

Supporting Information

Additional supporting information may be found online in the Supporting Information section at the end of the article.

Figure S1. Field photo showing (A) a cluster on an intertidal reef with the cluster measurement metrics, and (B) highlighting the live oysters, a box, and a shell, and the oyster height measurement of a live oyster.

Figure S2. (A) Oyster height size distribution comparison between Alligator Harbor (AH) and East Cove (EC) from collected clusters. “NS” indicates no statistical significance between groups using a Wilcoxon test ($P > 0.05$). Black points indicate outliers. (B–E) linear regression models of live oyster count and area of cluster for AH, $n = 14$, and EC, $n = 13$, (B, C) including oysters smaller than 2.5 cm

and (D, E) excluding oysters smaller than 2.5 cm. Black lines represent the regression lines, and the grey shading are the 95% CIs.

Figure S3. Comparison between Alligator Harbor (AH) and East Cove (EC). (A) Extracted cluster size distribution from the geospatial data for both sites. (B) Density per reef comparison. ****Indicates a statistical difference between groups conducted using a Wilcoxon test ($P < 0.0001$). Black points indicate outliers.

Figure S4. Histogram of cluster size distribution at East Cove (EC) for (A) 2022 and (B) 2023 split into 10 bins.

Figure S5. Comparison between 2022 and 2023 of East Cove (EC). (A) Extracted cluster size distribution from the geospatial data for both years. **Indicates a statistical

difference between groups conducted using a Wilcoxon test ($P < 0.01$). (B) Density per reef comparison for both years. NS indicates no statistical difference between groups conducted using a Wilcoxon test ($P > 0.05$). Black points indicate outliers.

Table S1. The respective live oyster, box, and shell quantities found within the clusters collected.

Table S2. The respective live oyster and box quantities found within the 625 cm² quadrats.

Table S3. Confusion matrix of ground truthing conducted at East Cove (EC) in 2023. The actual clusters were identified on the ground using a high-accuracy GPS. The predicted clusters were extracted using mean curvature from the digital elevation model.